Biol. Cybern. 84, 63–74 (2001)

Biological Cybernetics

Detection of simple radially symmetric targets: further evidence for the matched filter processing scheme in human pattern detection

U. Mortensen, G. Meinhardt

FB08, Westfälische Wilhelms-Universität, Fliednerstrasse 21, 48149 Münster, Germany

Received: 31 January 2000 / Accepted in revised form: 16 June 2000

Abstract. The detection of small radially symmetric targets was studied using a subthreshold summation paradigm. Small disc and disc-like patterns with diameters up to 0.6° were used for superposition on Bessel functions of zero order, subthreshold contrast and various spatial frequencies. Contrast interrelation functions prove linear over the whole range of contrasts used for the Bessel functions while their slopes show systematic variation with spatial frequency. An extrapolation of sensitivity from the slopes reveals that sensitivity can be predicted by a simple model assuming detection to be mediated by a transfer function made up as a cascade of an even bandpass function and the disc pattern spectrum, as has been found previously using one dimensional luminance distributions. Problems concerning the formation of pattern-specific radial symmetric filters are discussed.

1 Introduction

In this paper we report a detection experiment employing circular "discs" as stimuli and show that the sensitivity data can be explained with the matched filter model first proposed by Hauske et al. (1976). Data compatible with this model have been provided by Hauske (1974), Hauske et al. (1976, 1978) and by Meinhardt and Mortensen (1998), although for one-dimensional stimuli only. The matched filter model has often been criticized because of its alleged implausibility: if there existed matched filters for arbitrary patterns the number of such filters has to be astronomical. On the other hand, one may argue that such filters need not exist permanently in the visual system but may form during the detection process; it can be shown that e.g. Hebb's rule implies the formation of matched filters during the detection process (Oja 1982; Mortensen and Nachtigall 2000), although Hebb's rule is usually considered as representing processes of synaptic change that are too slow to allow for an immediate adaptation (e.g. Bauer and Dicke 1997); we return to this question in the Discussion. However, the change of synaptic connectivity is not necessarily involved when neuronal activity is organized during pattern detection (Aertsen et al. 1989). It remains to be shown that such activity mimics the mechanism of matched filtering of stimulus patterns or aspects of such patterns. The treatment of this question is left to future research; here we concentrate on the more simple question as to whether sensitivity data obtained for two-dimensional – in particular for radially symmetric patterns – are compatible with the notion of detection by matched filters.

From a mathematical point of view, radially symmetric patterns can be discussed like one-dimensional patterns, and so one may argue that the data presented in this paper do not yet allow a convincing test of the model for the case of two-dimensional patterns. So-called intrinsically two-dimensional patterns (Barth et al. 1998) like corners or crossings of lines or bars may provide more crucial data to be compared with the corresponding predictions of the matched filter model. It has been argued that a faithful representation of such patterns is not possible by linear filters (Zetzsche and Barth 1990). We return to this argument in the Discussion, after we have demonstrated the compatibility of the matched filter model, at least with data from radially symmetric stimuli.

2 Matched channels for radially symmetric patterns

2.1 The model

Let $s_t = s_t(x, y)$ be a two-dimensional luminance distribution with Fourier transform $S_t(u, v)$. Suppose there exists in the visual cortex some filter or "channel" C_t with unit response $g_t(x, y)$ to s_t (i.e. the response to a pattern with contrast equal to one), and g_t is maximal on

Correspondence to: U. Mortensen
(e-mail: mortens@psy.uni-muenster.de)

some subset $M_0 \subset \mathbb{R} \times \mathbb{R}$ compared to the responses to s_t of any other channel in the visual system. C_t will be called a matched channel for s_t. To further specify the matched channel, we make the following assumptions:

1. The matched channel is a cascade of two filters:
   (a) A radially symmetric pre-filter, characterised by a point-spread function (PSF) that is defined by the difference of two Gaussians (DOG-functions)
   $$h_0(x,y) = h_0(r) = A\mathrm{e}^{-ar^2} - B\mathrm{e}^{-br^2}, \quad \text{(PSF)} \qquad (1)$$
   $r = \sqrt{x^2+y^2}$.
   (b) A filter that is matched to the response g_{0t} of the pre-filter to s_t; this filter is characterised by the stimulus pattern, and by the PSF (1) – see below.
2. Suppose the matched channel C_t exists and the stimulus pattern is defined by the superposition $s = m_t s_t + m_b s_b$, with s_t a "test" pattern and s_b a "background" pattern. Let the unit responses of C_t to s_t and s_b be g_t and g_{tb}, respectively. Provided m_b is sufficiently small, the pattern $s = m_t s_t + m_b s_b$ is detected by C_t with probability p_0 if
   $$m_t g_t(r_0) + m_b g_{tb}(r_0) = c \ , \qquad (2)$$

where c is constant and r_0 is the position of the maximal response of C_t.

Assumption 1 caters to the fact that in all cases there is some filter preceding the matched filter, be it the lens of the eye. However, the site of the matched filter is most likely cortical, so that the pre-filter is constituted by the optical tract, possibly V1 or "higher" layers. The hypothesis of detection by a matched channel will be tested by estimating the system function of the channel. Therefore we need to know the system function corresponding to the PSF (1). The system function is given by the two-dimensional Fourier transform $H_0(u,v)$ of $h_0(x,y)$. Since h is assumed to have radial symmetry, H_0 is given by $H_0(u,v) = 2\pi\bar{h}_0(\omega)$, where the $\bar{h}_0$ is the Hankel transform $\bar{h}_0(\omega) = \int_0^\infty r h_0(r) J_0(\omega r)\mathrm{d}r$, with $J_0(x) = \int_{-\pi}^{\pi} \exp(ix\cos(\theta-\alpha))\mathrm{d}\theta$ the Bessel function of zero order (Papoulis 1981, pp. 141, 152), and $u = 2\pi f_1$, $v = 2\pi f_2$, $\omega = 2\pi f$, $f = \sqrt{f_1^2+f_2^2}$. Now since the Hankel transform of $\exp(-ar^2)$ is given by $\exp(-\omega^2/2a)$ (Papoulis 1981, p. 146), one has for the system function of the pre-filter

$$\bar{h}_0(\omega) = \frac{A}{2a}\mathrm{e}^{-\omega^2/4a} - \frac{B}{2b}\mathrm{e}^{-\omega^2/4a} \ . \qquad (3)$$

In order to compare the results of our experiment with the corresponding results of other authors, it will be interesting to consider the line spread function (LSF) corresponding to the PSF h_0. The LSF is defined to be the x-profile $\varphi(x) = \int_{-\infty}^{\infty} h_0(x,y)\mathrm{d}y$, and since $\int_{-\infty}^{\infty} \exp(-\alpha(x^2+y^2))\mathrm{d}y = \sqrt{\pi/\alpha}\exp(-\alpha x^2)$ (Papoulis 1981, p. 54), one has

$$\varphi(x) = A\sqrt{\frac{\pi}{a}}\,\mathrm{e}^{-ax^2} - B\sqrt{\frac{\pi}{b}}\,\mathrm{e}^{-bx^2} \quad \text{(LSF)} \ . \qquad (4)$$

It was said at the beginning of this section that the response of the postulated filter is maximal on some subset M_0 of $\mathbb{R} \times \mathbb{R}$. In the assumptions this subset was not specified further. It is shown in the Appendix that M_0 contains only a single point, namely $(0,0)$. If s_t has radial (circular) symmetry, then $s_t(x,y) = s_t(r)$. If the pre-filter has radial symmetry, then the response of the pre-filter to S_t is also radially symmetric, so that $g_{0t}(x,y) = g_{0t}(r)$; in the Appendix it is shown that the matched filter for the signal g_{0t} is also characterised by radial symmetry. The system functions are then defined by: (i) Hankel transforms $\bar{h}_0$ and $\bar{g}_{0t}$ of the (radially symmetric) PSF $h_0(r)$ of the pre-filter, and (ii) the matched filter tuned to the signal g_{0t}, respectively. Then (cf. Eq. A8), $\bar{g}_{0t} = \bar{h}_0\bar{s}_t$, and the matched channel has the system function

$$\bar{h}_t(\omega) = \alpha_{0t}|\bar{h}_0(\omega)|^2\bar{s}_t(\omega) \ , \qquad (5)$$

where α_{0t} is some proportionality constant related to the energy of the channel's response. Equation (5) represents the case in which the point of maximal output is $(x_0,y_0) = (0,0)$; a choice $(x_0,y_0) \neq (0,0)$, in particular the assumption that the response of the filter is maximal on a circle of radius $r_0 > 0$, leads to conceptual inconsistencies (for instance to the statement that the response $g_t(r)$ of the filter at any $r < r_0$ is not defined – see the Appendix).

If assumption 1 holds, the unit response of the matched channel to s_t at the position r is given by

$$g_t(r) = \begin{cases} \alpha_{0t}\int_0^\infty \omega\bar{h}_t(\omega)\bar{s}_t(\omega)J_0(r\omega)\mathrm{d}\omega, & r > r_0 = 0 \\ \alpha_{0t}\int_0^\infty \omega\bar{h}_t(\omega)\bar{s}_t(\omega)\mathrm{d}\omega, & r = r_0 = 0 \end{cases} \qquad (6)$$

(cf. (A7) in the Appendix) where J_0 is the Bessel function of order zero. The structure of the matched channel is given in Fig. 1.

Equation (1) in assumption 1 is more restrictive than is necessary for a test of the matched filter hypothesis; the characterisation of h_0 in terms of a DOG-function is not necessary to test the matched-channel hypothesis. In fact, for purposes of testing the hypothesis of detection by a matched channel it is sufficient to introduce some function representing the pre-filter, for instance a polynomial. However, assuming a DOG-function for the pre-filter ties our model to what is already known (or usually assumed) about early stages of visual processing (e.g. Kulikowski and King-Smith 1973; Hines 1976; Wilson 1978; Wilson and Bergen 1979; cf. Wilson et al.

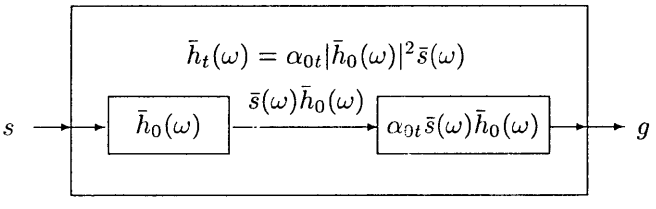

Fig. 1. The structure of a matched channel: the matched channel is a cascade of a pre-filter with system function $\bar{h}_0$ and a matched filter with system function $\alpha_{0t}\bar{s}(\omega)\bar{h}_0(\omega)$ (adapted from Meinhardt et al. 1998)

1990 for an overview of models on early visual processing).

Assumption 2 refers to superposition experiments (Kulikowski and King-Smith 1973, Hauske et al. 1976; Meinhardt and Mortensen 1998) as a means to test the model. To see how the test may be conceived let us suppose for a moment that the assumption 2 holds. Let us further assume that a matched channel C_t for s_t exists; if s_t is presented, then s_t will, in general, be detected by C_t. If the superposition $s = m_t s_t + m_b s_b$ is presented with m_b being small (the meaning of "small" is elaborated below), C_t will still be the maximally-activated channel, with response equal to $m_t g_t + m_b g_{tb}$. If the pattern s_b is chosen such that it represents an eigenfunction of C_t, the response g_{tb} of C_t will be proportional to the system function $\bar{h}_t$ of C_t. So if g_{tb} can be estimated from the data, this estimation can be compared with the prediction of $\bar{h}_t$ representing a matched filter for s_t; the details of this test are elaborated in Sect. 2.2.

Assumption 2 does not necessarily hold, so let us briefly look at some sufficient conditions for the assumption, justifying in particular (2) which implies a linear relation between m_t and m_b, at least as an approximation.

Let us suppose that there exist $n > 1$ channels $C_1, C_2, \ldots, C_n$ responding to the pattern s, and let $u_i = m_t g_{it} + m_b g_{itb}$ be the response of the i-th channel C_i, $1 \le i \le n$, with g_{it} the unit response of C_i to s_t, and g_{itb} the unit response of C_i to s_b. Suppose the probability of detection is given by $P(m_t, m_b) = 1 - \exp(-\sum_i |u_i|^p)$, with $p > 1$ a free parameter; the choice of this function is equivalent to the model of Quick (1974), which has become a sort of canonical model for probability summation or nonlinear pooling effects in visual modeling. Let u_t be the response of C_t, and suppose $u_t = \max(u_1, \ldots, u_n)$. There exists a $c \in \mathbb{R}$ such that if $P(m_t, m_b) = p_0$, then $\sum_i |u_i|^p = c$. As is well known, $\sum_i |u_i|^p \to u_t^p$ for $p \to \infty$, i.e. for p large the assumption of detection by a single channel and therefore (2) holds as an approximation. This allows one to say that "the value of p is large" is the assumption behind (2), implying that the relation between different values of m_t and m_b, i.e. the Contrast Interrelationship Function (CIF), should be linear to a reasonable degree of approximation (see Eq. 9). Generally, CIFs will be nonlinear (e.g. Meinhardt 1999; Logvinenko 1993). Now C_t will be the maximally-activated channel only if m_b is small; for larger values of m_b a channel responding optimally to the pattern s_b may become sufficiently activated to play a role on its own in the detection process and may in the end even dominate this process, implying again that the CIF will become nonlinear. Thus, (2) represents a linear approximation to the CIF only for "small" values of m_b.

The precise meaning of "small" for the contrast m_b is, however, difficult to define since it depends upon the sensitivity of the channels C_i to s_t and s_b. Therefore we approach the problem of small values for m_b pragmatically: we define $m_b = q m_t$, with $q < 1$. This way we can ensure that the contrast m_b will always be smaller than the threshold contrast for s_t, provided that the probability of detection equals some specified value $p_0 < 1$. The optimal values for q are: (i) sufficiently small such that the empirically determined CIF is linear to a fair degree of approximation, or (ii) sufficiently large to provide a range of possible m_b values allowing for a stable estimate of the parameters of the linear approximation (2). Further details about the choice of q and the estimation procedure are given in Sect. 3.4.

2.2 Testing the model

Before we outline the idea of the test we recall a general property of radially symmetric systems, namely the response to J_0 patterns, and relate them to the results of the preceding section.

Suppose that a matched channel C_t for s_t exists with system function $\bar{h}_t$ given by (5), and that assumption 2 holds. For such channels, Bessel functions of order zero are eigenfunctions, so if $s_b = J_0(2\pi f_0 r)$, then

$$g_{tb}(r; f_0) = \bar{h}_t(f_0) J_0(2\pi f_0 r) \ , \tag{7}$$

(Papoulis 1981, p. 152) where g_{tb} has been written as a function of f_0 instead of as a function of $\omega_0 = 2\pi f_0$ in order to facilitate the reference to the data[1]; correspondingly, $\bar{h}_t$ and $\bar{s}_t$ will also be written as functions of f_0 in the following. As shown in the Appendix, the response of C_t has to be assumed to be maximal at $r_0 = 0$, so that with respect to assumption 2 we only have to consider the case $r = 0$ in (7). Since $J_0(0) = 1$, (7) implies $g_{tb}(f_0) = \bar{h}_t(f_0)$, where we have dropped r for further simplification. Also, from (5):

$$\frac{g_{tb}(f_0)}{c} = \frac{\alpha_{0t}}{c} |\bar{h}_0(f_0)|^2 \bar{s}_t(f_0) = \frac{1}{c} \bar{h}_t(f_0) \ . \tag{8}$$

$g_{tb}(f_0)/c$ will be called the sensitivity[2] of the channel C_t.

The idea of the test is as follows. The pre-filter, defined by $\bar{h}_0$, is the same for all patterns s_t. As is obvious from (8), estimating the sensitivity $g_{tb}(f_0)/c$ allows estimation of $(\alpha_{0t}/c)|\bar{h}_0(f_0)|^2$ since the $\bar{s}_t(f_0)$ are known, and these estimates may be used to find an estimate of $\bar{h}_0(f_0)$. Equation (8) further suggests that multiplying this estimate with the known Hankel transform $\bar{s}_t(f_0)$ of s_t leads, after correction with some factor corresponding to α_{0t}/c, to predictions of $g_{tb}(f_0)$. The test of the model then consists of a comparison of estimated and predicted sensitivities.

2.2.1 Estimating the sensitivities. Now (2) implies

$$m_t = \frac{c}{g_t} - m_b \frac{g_{tb}}{g_t} = \alpha^t + \beta^t m_b \ , \tag{9}$$

with $\alpha^t = c/g_t$ and $\beta^t = g_{tb}/g_t$.

[1] Writing f_0 instead of ω_0 requires, of course, the introduction of new function names. However, we keep the original function names to avoid a more cumbersome notation.

[2] Usually, the sensitivity is the reciprocal $1/m(f_0)$ of the threshold contrast $m(f_0)$ of a sinusoidal grating with spatial frequency f_0. If the grating is detected by a linear channel with system function $H(f_0)$, then the sensitivity is proportional to $|H(f_0)|$. In our case $H(f_0) = |H(f_0)| = 2\pi \bar{h}_t(f_0)$, which motivates our term "sensitivity".

For a given pattern s_t and given spatial frequency parameter f_0 specifying $s_b = J_0(2\pi f_0 r)$, the estimates $\hat{\alpha}^t$ and $\hat{\beta}^t$ of the regression parameters are determined from experimentally determined CIFs; details are given in Sect. 3.4. $\hat{\beta}^t$ is an estimate of g_{tb}/g_t, so

$$\frac{\hat{\beta}^t}{\hat{\alpha}^t} = \hat{g}_{tb} \cong \frac{g_{tb}}{c} \quad , \tag{10}$$

where "$\cong$" stands for "is an estimation of".

2.2.2 Predicting the sensitivities. From (8),

$$\sqrt{\frac{1}{c}\frac{g_{tb}(f_0)}{\bar{s}_t(f_0)}} = A_{0t}|\bar{h}_0(f_0)|, \quad A_{0t} = \sqrt{\alpha_0/c} \quad . \tag{11}$$

Substituting $\hat{g}_{tb}$ (10) for g_{tb}/c we introduce

$$\bar{h}^t_{0,\mathrm{est}}(f_0) \stackrel{def}{=} \sqrt{\frac{\hat{g}_{tb}(f_0)}{\bar{s}_t(f_0)}} \quad . \tag{12}$$

$\bar{h}^t_{0,\mathrm{est}}$ is an estimate of $\bar{h}_0$, derived from the data for the stimulus pattern s_t. Equation (12) is the analogue of (11), and consequently we may write $\bar{h}^t_{0,\mathrm{est}} \cong A_{0t}\bar{h}_0$, so $\bar{h}^t_{0,\mathrm{est}}$ can differ from $\bar{h}_0$ because A_{0t} may assume different values for different patterns. The estimates $\bar{h}^t_{0,\mathrm{est}}$ will be used to estimate the parameters A, B, a and b of the pattern-independent pre-filter function $\bar{h}_0$ as defined in (3); this will imply some implicit averaging of the proportionality constants A_{0t}. Let

$$\bar{h}_{0,\mathrm{est}}(f_0) = \frac{\hat{A}}{2\hat{a}}\mathrm{e}^{-\omega^2/4\hat{a}} - \frac{\hat{B}}{2\hat{b}}\mathrm{e}^{-\omega^2/4\hat{a}} \tag{13}$$

be the estimate of $\bar{h}_0$ as defined in (3), with $\hat{A}$, $\hat{B}$, $\hat{a}$ and $\hat{b}$ estimates of A, B, a and b. Let $g^{\mathrm{est}}_{tb}(f_0)$ denote the sensitivity predicted by the matched filter model for the stimulus pattern s_t and the spatial frequency f_0. Then

$$g^{\mathrm{est}}_{tb}(f_0) = \hat{A}^2_{0t}|\bar{h}_{0,\mathrm{est}}(f_0)|^2\bar{s}_t(f_0) \quad , \tag{14}$$

where the $\hat{A}^2_{0t}$ are pattern-specific adjustments to $|\bar{h}_{0,\mathrm{est}}(f_0)|^2$ corresponding to the $A^2_{0t} = \alpha_{0t}/c$; the $\hat{A}^2_{0t}$ are the only estimates of free parameters required when the sensitivities for the individual stimulus patterns are fitted according to the matched filter model – apart from the parameters A, B, a and b characterising the system function $\bar{h}_0$ of the pre-filter. However, these latter parameters are the same for all single- and double-disc patterns used.

3 Experiments

3.1 Subjects

Two subjects (KF and RF, male, 24 and 25 years of age) took part in the experiment. KF is a corrected myope, while RF has natural eyesight. Both subjects are well acquainted with psychophysical experiments, in particular those involving detection. KF took the measurements for all experimental conditions and RF performed control measurements to confirm the basic results of the experiment.

3.2 Apparatus

Patterns were generated using a VSG2/3 stimulus generator and displayed on a VM3640 grey-scale monitor. A pattern was scaled in contrast using a scaling table loaded with 512 entries equidistant in contrast, where entry No. 511 pointed to the pattern in maximum contrast and entry No. 0 pointed to the pattern in zero contrast. Each of the 512 scaling entries referred to a lookup table which was a linear grey staircase consisting of 256 steps chosen from a palette of 4096 possible grey values, the median value (128) always referring to grey value No. 2048. The relationship between the grey level entries 0 to 4095 and the luminance on the screen was linearized by means of RGB translation tables. This linearity was checked before each experimental session using a calibration program that determined the relationship between the digitized grey values of the VSG2/3 and luminance on the monitor (in $\mathrm{cd/m})^2$ as measured by an LMT 1003 photometer. The coefficient of determination of the regression line was in all cases greater than 0.98. The refresh rate of the monitor was 72 Hz at a horizontal frequency of 39 kHz, and the pixel resolution was set to 640×480 pixels. The room was darkened so that the ambient illumination approximately matched the luminance on the screen. The mean luminance of the screen was set to 50 $\mathrm{cd/m}^2$. Patterns were viewed monocularly at a distance of 170 cm. The subjects used a chin rest and an ocular limiting the visible area of the screen to a circular field of 4.6° in diameter.

3.3 Stimuli

3.3.1 Contrast sensitivity function. Kelly and Magnuski (1975) found that the contrast sensitivity function determined with Bessel functions of zero order, i.e. with $J(2\pi f_0 r)$, differ from those determined with sinusoidal gratings. Since J_0 patterns were employed as background patterns, the contrast sensitivity function for such patterns was determined first in order to determine the range of spatial frequency parameters f_0 to be used. Stimulus patterns where defined as

$$s(r; f_0) = mJ_0(2\pi f_0 r), \quad r \leq 4^\circ \quad , \tag{15}$$

with $m = (l_{\max} - l_{\min})/2l_0$ (Maxwell contrast).

3.3.2 Superposition experiment. As shown in Fig. 3 the stimulus patterns were defined according to

$$l(r) = l_0(1 + m(s_t(r) + qs_b(r)) \quad , \tag{16}$$

where l defines luminance and l_0 the space-average luminance of the screen, and m again representing Maxwell contrast. $s_t(r)$ specifies the test pattern. The background pattern is given by $s_b(r) = s(r)$ as defined in (15). Two types of stimulus patterns, the single-disc and

the double-disc, patterns, were employed. For single-disc patterns, the function s_t represents a single circular "disc" with radius R (visual angle):

$$s_t(r) = \begin{cases} 1, & r \le R_k \\ 0, & r > R_k \end{cases} \quad k = 1, \ldots, 4 \tag{17}$$

Note that we should write s_{tk} in the following, since a stimulus pattern is defined with respect to a particular radius R_k. Since confusions cannot occur, we will continue to write s_t to keep the notation simple.

For double-disc patterns, the function $s_t(r)$ is defined as the concentrical superposition of two circular discs having different radii and luminance:

$$s_t(r) = (1+\gamma)s_{t1}(r) - \gamma s_{t2}(r), \quad \gamma = 1/2 \tag{18}$$

where the individual discs are given by

$$s_t(r) = \begin{cases} 1, & r \le R_k, \\ 0, & r > R_k, \end{cases} \qquad k = 1, 2 \ . \tag{19}$$

The Hankel transform of a single-disc pattern s_t is given by

$$\bar{s}_t(\omega_0) = \frac{R_k J_1(R_k \omega_0)}{\omega_0} \ , \tag{20}$$

where J_1 denotes a Bessel function of order one (Papoulis 1981, p. 147). The radii of the single-disc patterns were $R_1 = 0.075°$, $R_2 = 0.15°$, $R_3 = 0.2°$, or $R_3 = 0.3°$. These values were chosen so as to maximise the sensitivity of the test of the model, namely such that the corresponding spectra, i.e. the transforms (20), for some values of f_0 assume positive – for others negative – values.

There was only a single double-disc pattern; the radii of the individual discs were $R_1 = 0.075°$ and $R_2 = 0.25°$. The Hankel transform of the double-disc pattern is given as

$$\bar{s}_t(\omega_0) = (1+\gamma)\bar{s}_{t1}(\omega_0) - \gamma \bar{s}_{t2}(\omega_0) \ , \tag{21}$$

and the $\bar{s}_{tk}(\omega_0)$, $k = 1, 2$ are defined by (20).

A pattern s_t – be it a single- or double-disc pattern – was superimposed upon a radially symmetric Bessel function of zero order truncated at 4°, i.e. the Bessel function was large compared to the test stimuli. Figure 2 illustrates the single-disc stimulus patterns used in the experiment.

3.4 Procedure

3.4.1 Contrast sensitivity. The spatial frequencies $\{1, 2, 3, 4, 5, 6$ c/deg$\}$ were employed. Let $g(f_0) = m(f_0)J_0(2\pi f_0 r)$ be the response to the J_0 pattern. The stimulus is assumed to be detected – corresponding to assumption 2 in Sect. 2.1 – if $g(f_0) = c$, c a constant reflecting the strength of the channel's response at which the stimulus is detected with probability p_0 (see Eq. (2)). The threshold contrast $\bar{m}(f_0)$ was determined according to the procedure Sect. 3.4.3; the contrast sensitivity for the spatial frequency f_0 is defined as $1/\bar{m}(f_0)$.

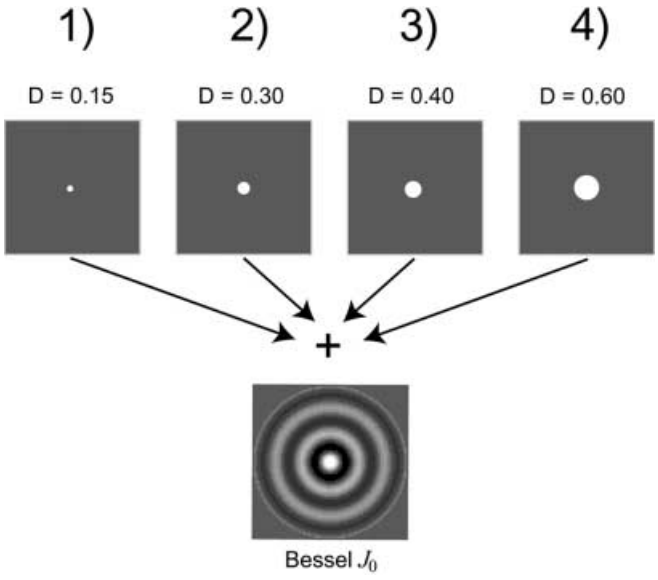

Fig. 2. Illustration of the test and background stimuli used for superposition in the experiment. Four simple bright disc patterns were used for superposition with Bessel type (J_0) background stimuli of large spatial extent. The J_0 luminance distributions were 4° in diameter; the diameters ($D_k = 2R_k$) of the disc patterns are listed. The figure correctly reflects the size relationships between test patterns and background

3.4.2 Superposition experiments. Within an experimental session the contrast thresholds for the compound patterns (superpositions of the test pattern on Bessel functions of zero order at each of the six possible spatial frequencies) and the test pattern alone were determined. For each spatial frequency f_0 of the background pattern s_b, four values of q were employed to estimate the linear approximation to the contrast interrelation function corresponding to the value of f_0. These values were $q_1(f_0)$, $q_2(f_0)$, $-q_1(f_0)$, $-q_2(f_0)$; where $q_2 = q_1/2$, and negative factors of q denote the case that $-qJ_0(ar)$ was presented as the background pattern (contrast reversal technique, Kulikowski and King-Smith 1973). The factor $q_1(f)$ was always chosen such that the relative component strength of the Bessel function was not greater than 40% of its threshold contrast. In order to determine the appropriate values of q for each spatial frequency of the Bessel function, measurements of both the thresholds for simple J_0 targets and of the testpatterns s_t without background pattern were carried out prior to measuring the thresholds of the single- or double-disc stimulus patterns. The estimation of the threshold contrasts of J_0 patterns also served to determine the proper range of the spatial frequencies for the superposition experiment. In agreement with Kelly and Magnuski (1975) we found that the contrast sensitivity function (CSF) for radially symmetric Bessel targets is shifted towards lower frequencies as compared to a CSF obtained with sinusoidal gratings (see Fig. 3). According to this result and the properties of the spectra for the single-disc patterns (cf. Fig. 6) we selected the the spatial frequencies f_0 $\{1, 1.5, 2, 3, 4, 5$ cyc/deg$\}$ for the background pattern s_b. For the experiment employing

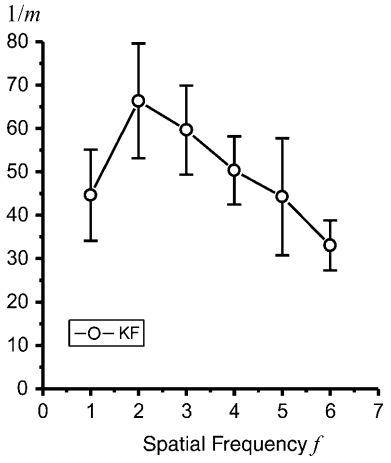

Fig. 3. Contrast sensitivity function, measured with radially symmetric Bessel targets of 4° diameter. Error bars show the standard deviation. The function peaks at a spatial frequency of $f = 2$ cyc/deg and is thus shifted towards lower frequencies compared to contrast sensitivities measured with sinusoidal grating targets (cf. Campbell and Robson 1968)

the double-disc pattern the spatial frequencies $\{1, 1.5, 2, 2.5, 3, 3.5$ cyc/deg$\}$ were selected, again taking also the spectrum of the double-disc pattern into account (cf. Fig. 9). For each experimental session the computer generated a random list of all superimposed patterns, i.e. the subject was not able to generate valid hypotheses about the sequence of spatial frequencies of the superimposed patterns nor the actual radius of the disc targets. Contrast thresholds were determined employing the method of limits as follows.

3.4.3 Determination of thresholds. The initial contrast was set to a starting value well above threshold. The subject pressed a button (button 1) on a small response keyboard to start the first down-run (decrementing the starting value). The total number of possible decrements comprised 512 contrast steps (equidistant in contrast), each of them with a contrast amplitude of 3.9×10^{-5} Maxwells and 24 ms duration. The image was always present on the screen, i.e. there was no temporal gating from one contrast step to the next (rectangular temporal staircase). When the stimulus was, at some value m_{down}, no longer visible to the subject she or he pressed another button (button 2) on the response keyboard. The value m_{down} was then further reduced by 25%. The subject now started an incremental staircase by again pushing button 1; the incremental steps were of the same amplitude and duration as the decremental steps. When the pattern became visible, i.e. when the pattern was barely distinguishable from the screen background, at some contrast m_{up}, the subject signaled this event by again pushing button 2. The threshold contrast was defined as the arithmetic mean $\bar{m} = (m_{\text{up}} + m_{\text{down}})/2$; $\bar{m}$ is called a threshold measurement.

At least twelve threshold measurements were carried out for each value of q for each compound pattern (i.e. a stimulus pattern superimposed on a background pattern). From the second measurement onwards, the starting value of a threshold measurement was taken as the mean of the foregoing threshold measurements. Generally, the subjects were advised to press the button if they had the impression that the screen deviated in any way from the mean pale grey, or turned to pale grey again, respectively. They then fixated on the center of the screen, which was marked by a small permanent dot. One experimental session, lasting about three hours including short recovery breaks, was carried out per day. The experimental sessions were conducted over at five consecutive days.

4 Results

4.1 Contrast sensitivity

The results of the contrast sensitivity measurements are shown in Fig. 3. As stated above, the data comply with the findings of Kelly and Magnuski (1975).

4.2 Estimation of the pre-filter

The parameters of the pre-filter $\bar{h}_0$ were estimated from the single-disc data; the same estimate $\bar{h}_{0,\text{est}}$ of $\bar{h}_0$ was used to predict the sensitivities for the single-disc and for the double-disc data. The estimates $\hat{g}_{tb}$ of g_{tb} were determined according to (10), and the estimates $\bar{h}^t_{0,\text{est}}$ were determined according to (12), i.e. $\hat{g}_{tb}(f_0) = \hat{\beta}^t(f_0)/\hat{\alpha}^t$. The corresponding CIFs could indeed be considered linear for the chosen range of background contrasts; the CIFs for the four single-disc patterns cannot be shown due to lack of space, so, in order to provide an illustration, we restrict ourselves to Fig. 8, which shows the CIFs for the double-disc data.

For certain stimuli there exist spatial frequencies for which $\bar{s}_t(f_0) = 0$ (see Fig. 6) so that in these cases the ratio $\hat{g}_{tb}/\bar{s}_t$ is not defined. Accordingly, for the frequencies $f_0 = 2.0$ and $f_0 = 4.0$ the stimulus defined by the radius $R_2 = 0.15°$ could not be considered. Likewise for $f_0 = 3.0$ the stimulus defined by the radius $R_3 = 0.2°$ and for the frequency $f_0 = 4.0$ the pattern defined by the radius $R_2 = 0.15°$ were not considered in the estimation of $\bar{h}_0$. The individual estimates $\bar{h}^t_{0,\text{est}}$ together with the fitted $\bar{h}_{0,\text{est}}$ are given in Fig. 4. The parameters[3] of $\bar{h}_{0,\text{ext}}$ are given in (22).

$$\begin{aligned} \hat{A} &= 22421.9 \quad \hat{B} = 13963.8 \\ \hat{a} &= 89.1564 \quad \hat{b} = 57.0774 \end{aligned} \tag{22}$$

It is of interest to compare $\bar{h}_{0,\text{est}}$ with estimates reported in the literature As pointed out in Sect. 2.1, one may consider the LSF $\varphi(x)$, i.e. the x-profile of the PSF

[3] The parameters were estimated using the Levenberg-Marquardt algorithm (Press WH, Teukolsky SA, Flamery BP, Vetterling WT (1996) Numerical Recipes in Pascal. Oxford University Press, Oxford) as implemented in Mathematica, version 3.0. The algorithm provides nonlinear least squares estimates, based on a steepest descent method of minimising $\chi^2(\vec{a}) = \Sigma_i((\bar{h}^t_{o,\text{est}}(f_i) - \bar{h}_{0,\text{est}}(f_i;\vec{a})/\sigma_i)^2$, with $\vec{a}$ the vector of parameters A, B, a and b, and σ_i^2 the variance of the $\bar{h}^t_{0,\text{est}}(f_i)$.

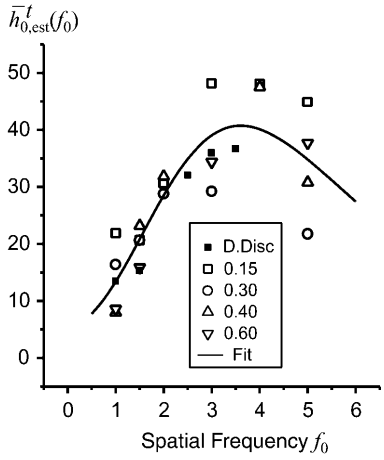

Fig. 4. Estimates $\bar{h}^t_{\mathrm{est}}$ of the system function characterising the pre-filter according to (12). The variance of the estimates increases with spatial frequency, indicating that the matched-filter model may require specific adjustments for each test pattern. The solid line represents $\bar{h}_{0,\mathrm{est}}$ as defined in (13)

$h_0(x,y)$. Figure 5 shows the LSF corresponding to $\bar{h}_{0,\mathrm{est}}$ in Fig. 4, i.e. $\varphi(x)$ as given in (4) with parameters $\hat{A}$, $\hat{B}$ etc. as given above. The retinal coordinates (x-axis) are given with respect to two units: degrees (bottom axis) and minutes (top axis), to allow easy comparisons with the data presented by Wilson (1978) and Wilson and Bergen (1979), and Hines (1974), respectively. The data of Hines (1976), Wilson (1978) and Wilson et al. (1979) indicate a minimum of sensitivity, i.e. a minimum of the inhibitory trough, close to 0.1 degrees or, equivalently, 5 and 6 min of arc, while the minimum predicted by our LSF is closer to 0.2 degrees, i.e. at 9 min of arc. Hines (1974) fitted the function

$$\mathrm{LSF}(x) = A'/(\sigma_a\sqrt{2\pi})\exp(-x^2/2\sigma_a^2) - B'/(\sigma_b\sqrt{2\pi})\exp(-x^2/2\sigma_b^2)\ ,$$

so with respect to the parameters A, B, a and b in (4), we get

$$A' = A\pi/a, \quad B' = B\pi/b$$
$$\sigma_a^2 = 1/2a, \quad \sigma_b^2 = 1/2b$$

implying $A' = 125.745$, $B' = 122.232$, $\sigma_a = .0749$ and $\sigma_b = .0936$, from our estimates in (22). Hines estimated $\sigma_a = 0.039$, $\sigma_b = 0.058$. In our case, the sensitivity at 0° assumes the value 933°, while in Hines' measurements a value of about 650° results.

Considering the possibility of differences between individual subjects and the different experimental conditions under which LSFs were determined, the correspondence between our LSF and the one determined by the mentioned authors is sufficiently good to accept our estimate of the LSF $\varphi(x)$ and therefore of $\bar{h}_0$.

4.2.1 Sensitivities and the test of the matched-filter model. Let us first consider the sensitivities for the single-disc patterns. If the matched-filter model holds they should correspond to the corresponding predictions. The sensitivities predicted for a given pattern s_t were calculated according to (14). Figure 6 shows the Hankel transforms $\bar{s}_t$ for the individual single-disc patterns (17).

The empirical sensitivities together with the predictions by the matched filter model, are shown in Fig. 7. The proportionality constants $\hat{A}^2_{0t} = \hat{A}^2_{0k}$, estimated for each individual pattern (radius R_k, $1 \le k \le 4$), were $\hat{A}^2_{01} = 1.30811$, $\hat{A}^2_{02} = 0.856$, $\hat{A}^2_{03} = 1.14893$ and $\hat{A}^2_{04} = 0.5875$, respectively.

The sensitivity data agree well with the predictions (cf. Eq. 8), based on the spectra of the test patterns and the estimated pre-filter function; note that the positions of the zero crossings of the test pattern spectra agree closely with those of the sensitivity data. Note that the matched filter prediction (14) for the sensitivity is a product of the test pattern's spectrum and the system function of the pre-filter. Consequently, the zero crossings of the spectra and the zero crossings of the matched filter prediction must coincide. The empirical sensitivity data are in all cases close to these positions, i.e. the

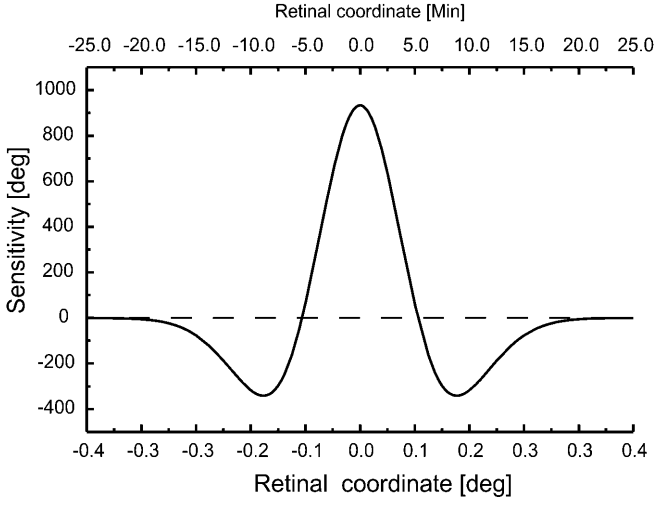

Fig. 5. The line spread function (4) corresponding to the estimated pre-filter function $\bar{h}_{0,\mathrm{est}}$ shown in Fig. 4

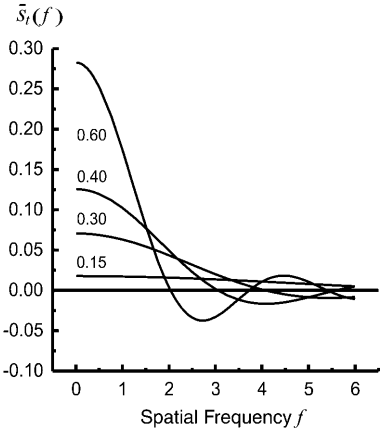

Fig. 6. Spatial frequency spectra of the single-disc test patterns. The disc diameters ($2R_k$) are listed for each plots. The spectra differ sufficiently from each other to allow for sensitivity estimates that differentiate well between patterns (see Fig. 7)

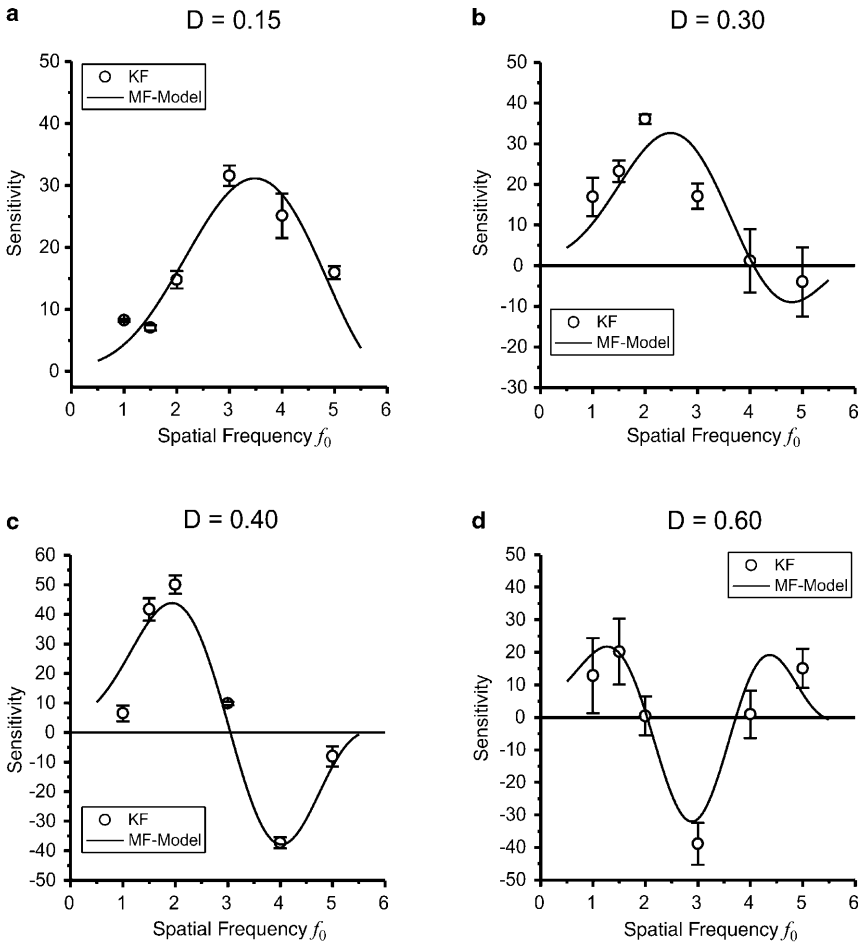

Fig. 7. Sensitivities of the postulated matched channels for four discs of different diameters, depending upon the spatial frequency f_0 of the background pattern $s_b = J_0(2\pi f_0 r)$. The error bars represent the standard error of the slope estimate of the corresponding contrast interrelation functions (CIFs). The solid lines are the predictions of the matched channel model (5) (see Sect. 2 for explanation). Data from subject KF

matched channel model predicts the locations of zero sensitivity correctly.

The estimates $\hat{A}^2_{0k}$ will somehow depend upon the proportionality constants α_{0t}/c, as equation (11) suggests. The fact that constants $\hat{A}^2_{0k}$ are needed for each radius R_k suggests that the values of either c or α_{0t}, or possibly both, vary with disc size. Since the values of $\hat{A}_{0k}$, are not monotonically related to the R_k we suggest that the value of the internal threshold is set randomly for a given disc size.

Figure 8 shows CIFs for the stimulus pattern s_t for the double-disc data as defined in (18) and (19). The data are shown for subject KF but are qualitatively the same for subject RF. For all values of the spatial frequency f_0, the corresponding CIF can be well approximated by a linear function (small derivations occur at $f_0 = 2.0$ cyc/deg) as determined by linear regression, with a slope depending upon the value of f_0.

The empirical sensitivities $\hat{g}_{tb}$ were estimated as before, according to (10), and the predicted sensitivities $g^{\text{est}}_{tb}(f_0)$ again according to (14). Recall that the same parameter estimates (22) for A, B, a and b characterising the pre-filter $\bar{h}_0$ (cf. Eq. 3) – and estimated from the threshold data for the single-disc patterns – were employed for the double-disc patterns. Therefore, except for a proportionality factor $\hat{A}^2_{0t}$, no free parameter was estimated to fit the model to the data. As may be seen from Fig. 9, the matched filter model exactly predicts the position of the zero crossing in the sensitivity data and yields a smooth function which altogether describes the data correctly.

5 Discussion

The main purpose of this paper is to show that the matched filter model (Hauske et al. 1976, 1978; Meinhardt and Mortensen 1998; Mortensen and Nachtigall 2000) is compatible with data from detection experiments with two-dimensional, in particular radially-symmetric "single disc" and "double disc" patterns. The matched filter model may be considered a special-case of the the cell assembly model proposed by Mortensen and Nachtigall (2000). They show that Hebb's rule, stabilised so as to prevent the infinite growth of synaptic weights, implies that a neuron adapting according to this rule is transformed into a matched filter for that part of the stimulus pattern that covers its receptive field; the neuron will be a matched filter for the pattern if the pattern fits into the receptive field of the neuron. The theoretical background of our approach is therefore: (i) that the visual system is highly adaptive, and (ii) is linear for contrasts at threshold level. The cell assembly model proposed in Mortensen and Nachtigall (2000) was not fitted to the data reported here since it: (i) requires the fitting of an additional free

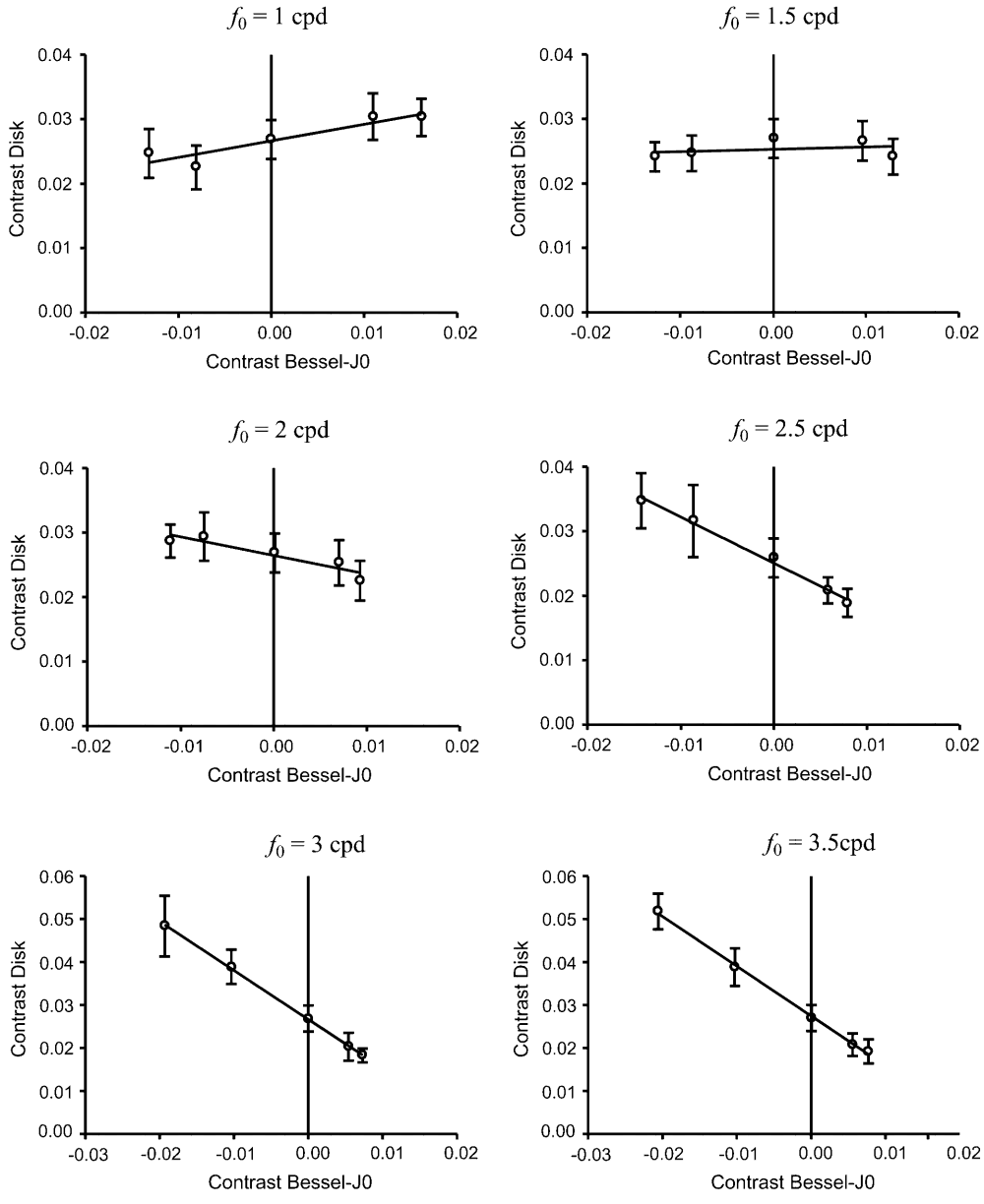

Fig. 8. Examples of CIFs for different values $f = f_0$ of the Bessel function $m_b J_0(2\pi f_0 r)$ employed as pattern s_b upon which the double-disc pattern (18) was superimposed upon a for small values of m_b. Data from subject KF

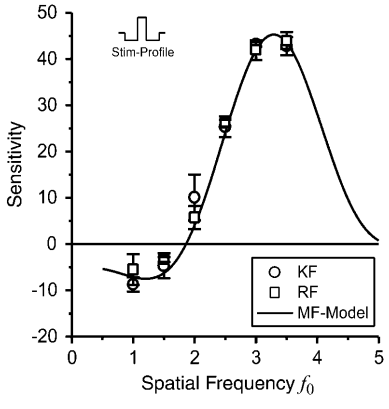

Fig. 9. Sensitivities for the double-disc pattern superimposed upon a Bessel function $J_0(2\pi f_0 r)$ for different values of f_0. The luminance profile of the test pattern is indicated by the symbols. Data are shown for two subjects, the details are as in Fig. 7. The key shows the luminance profile of the test pattern

parameter representing the size of the adapting receptive fields, and (ii) our data agree already with the more parsimoneous matched filter model.

Up to now, two-dimensional patterns do not seem to have been employed in tests of the matched filter model. The model has been formulated with respect to radially-symmetric patterns since such patterns have the great advantage of drastically reducing the experimental costs of superposition experiments because the background (J_0) pattern depends on only a single spatial frequency pattern; however, the generalisation to two-dimensional patterns that are not radially symmetric is straightforward, and further experiments with different two-dimensional patterns are required to evaluate the validity of the model.

One may, however, start modeling coding processes from quite a different angle. One well known and equally well discussed approach is to assume probability summation or nonlinear pooling of elementary linear chan-

nels (Quick 1974; Graham 1977; Wilson and Bergen 1979; see also Graham 1989 for a review) commented upon in Sect. 2.1; this line of attack to pattern detection has already been discussed in Mortensen and Nachtigall (2000). Here, we will look at an alternative explanation.

To begin with, the structure of our brains is – most likely – the result of an evolutionary process, and the type of neurons in the visual system as well as their wiring should somehow correspond to the statistics of visual scenes of our environment (Field 1987). Furthermore, the neural machinery should be robust in the sense that the loss of certain neurons can be compensated for by the activity of other neurons, meaning that features should not be coded by single neurons. An arbitrary scene should be represented with sufficient fidelity. Additionally, one may invoke the principle of reduction of redundancy (Barlow 1961): a visual scene should, according to this principle, be represented by "the activity of a sparse selection of reliable and nonredundant (i.e. independent) elements" (Barlow 1983), or, as Zetzsche et al. (1993) put it, "the correlations between the coding of the input symbols should be such that the signal is reproduced at a given level of quality with the minimum data possible".

Zetzsche and Barth (1990) introduced the notion of intrinsic dimensionality of signals (or parts of signals) to characterise certain types of statistical dependencies among inputs:

1. 0D-signals: strong isotropic signals with approximately constant statistical dependencies, representing homogeneous interior regions.
2. i1D-signals, i.e. intrinsically one-dimensional signals, characterised by strong anisotropic dependencies related to orientations (e.g. edges).
3. i2D-signals i.e. intrinsically two-dimensional signals; such signals cannot be represented by 0D- or i1D-signals. i2D-signals are, for instance, corners, or crossing line elements.

As Zetzsche et al. (1993) and Zetzsche and Krieger (1999) point out, i2D-signals are a statistical minority and thus play an important role in the reduction of redundancy. Curved lines are an example of i2D-signals; from an information theoretical point of view curved features play a very important role in the process of identifying a pattern: Attneave (1954) already argued that it is the extrema of curvature that provide most information about the identity of a pattern.

Zetzsche and Barth (1990) and Zetzsche and Krieger (1999) argued that linear models – for instance of curvature detection by end-stopped cells – may lead to false responses due to the defining characteristic of linear systems, namely the logical OR-operation: the activity of a linear system can always be represented as a superposition of i1D-eigenfunctions, and any of them can lead to a non-zero response of the system. This means in particular that a linear detector for a two-dimensional (sub-)pattern can in principle be activated by an i1D-signal. Zetzsche and Barth (1990) therefore conclude that i2D-detectors should be defined by logical AND-operator; they provide a detailed discussion of such operators in terms of a non-linear wiring of end-stopped cells, and Zetzsche and Krieger (1999) discuss such detectors with respect to the statistics of natural scenes. Saito et al. (1988) discuss AND-operators with respect to dot-responsive cells which may also play a role in the detection of the radially-symmetric stimuli employed in our experiments. Further, Barth et al. (1998) showed that textures cannot be identified if the identification mechanism is based on the evaluation of energy measures since power spectra do not necessarily differentiate between different texture patterns; it follows that the nonlinear i2D-operators should be related to higher than second-order statistics of the input pattern. The notion of reduction of redundancy together with the arguments for the nonlinearity of neural units for i2D-signals or features represent quite a challenge for the matched filter and therefore for the cell assembly model of Mortensen and Nachtigall (2000); after all, the matched neurons are conceived as linear devices, and since matched filters may be linked to a principal component type of analysis of the visual input (Oja 1982; Linsker 1986a,b; Sanger 1989, 1990) they rely on detection and identification on the basis of second-order statistics.

However, we are dealing with data from detection experiments where stimuli are presented with small, i.e. near-threshold contrasts. Experiments of the sort reported here define what has been called by Zetzsche and Krieger (1999) a "deliberately impoverished environment", leading, in their eyes, to an inadequate conception of the neural units involved. On the other hand, our findings may reflect the activity of linearised versions of i2D-filters, and detection experiments may actually be useful in exploring the properties of such filters. Apart from this, threshold experiments may be useful to further explore some aspects of the principle of redundancy reduction: as van Hateren (1992) pointed out, redundancy reduction is most likely counterproductive in cases of low stimulus intensities because such a reduction may imply spatial and temporal fluctuations, spatial pooling and temporal integration. This could mean that the characteristics of stimulus processing depend upon the conditions of the stimulus presentation, and the formation of matched filters or matched neurons could be typical for visual processes that are specific for the case of low contrasts; it is not clear why possible processes of this sort should not be investigated.

Another, almost standard argument against the matched filter model refers to combinatorial problems: it is argued that if feature aspects are to be coded by corresponding matched filters a huge number of such filters has to exist, and additional processes have to be postulated that decide which combination of activated matched filters gives the best match (Zetzsche et al. 1993). However, an aspect of stimulus processing that is usually not considered in models of coding based on redundancy reduction and on the statistics of natural scenes is fast adaptivity. As pointed out in Mortensen and Nachtigall (2000) matched neurons may result from fast adaptation of neurons to stimuli. Gerstner et al. (1993) proposed a spike rate (SR) model according to which information is coded in terms of the timing of

spikes (activation potentials), and neurons adapt according to Hebb's rule at a very fast rate. Ritz et al. (1994) showed how the SR model may be employed to discuss feature linking and pattern segmentation processes, so the changing of synaptic weights according to Hebb's rule does not necessarily imply that adaptation is slow. Kistler and van Hemmen (1999) further discussed, within the framework of the SR model, short-term neural plasticity with respect to coherently firing neurons. Consequently, one could think of embedding the adaptive Hebb model of Mortensen and Nachtigall (2000) into an SR-type model. Such an embedding would also provide a link to the finding that attentional and learning processes influence the coding of stimulus patterns even in area V1 (Gilbert et al. 2000; Martinez-Trujillo and Treue 2000). Together with the above-mentioned possibility that the good fit of our linear two-dimensional filters reflects the linearised activity of nonlinear i2D-filters, the possibility that such filters form by fast-adapting processes may well be considered. Adaptivity and the principle of reduction of redundancy need not exclude each other; instead, these aspects of the functioning of the visual system may complement each other.

Appendix: Derivation of the system function

We consider the matched filter for a single two-dimensional input pattern $\sigma = ms$, where m denotes contrast and $s = s_t(x,y)$ represents a two-dimensional luminance distribution. Let $S(u,v)$ be the Fourier transform of s and $H(u,v)$ the system function of the detecting channel; H is the Fourier transform of the PSF $h(x,y)$. The response of the channel is given by

$$g(x,y) = m g_t(x,y) = \frac{m}{4\pi^2} \iint_{-\infty}^{\infty} S(u,v) H(u,v) \mathrm{e}^{i(ux+vy)} \mathrm{d}u \, \mathrm{d}v \ ; \qquad \text{(A1)}$$

g_t is the unit response, i.e. the response for the contrast $m = 1$. The filter is matched to the pattern with Fourier transform S if

$$H(u,v) = \alpha S^*(u,v) \mathrm{e}^{-i(ux_0+vy_0)} \ , \qquad \text{(A2)}$$

where S^* is the complex conjugate of S and α is a parameter allowing adjustment of the energy to a prespecified value (Papoulis 1981).

Suppose now that s has radial symmetry, i.e. $s(x,y) = s(r)$. Equation (24) suggests that the PSF h, of which $H(u,v)$ is the Fourier transform, is also radially symmetric, i.e. $h(x,y) = h(r)$. Suppose $(x_0,y_0) \neq (0,0)$; the circular symmetry of s suggests the postulation that (x_0,y_0) is a point on a circle with radius $r_0 = \sqrt{x_0^2 + y_0^2} > 0$; it will be shown that this postulate is inconsistent with the idea that the detecting filter is matched to s.

Let us introduce polar coordinates for x, y, x_0, y_0, u and v, i.e. $x = r\cos\omega$, $y = r\sin\omega$, $x_0 = r_0\cos\omega$, $y_0 = r_0\sin\omega$, $u = \omega\cos\phi$, $v = \omega\sin\phi$, and let $\bar{h}(\omega)$, $\bar{s}(\omega)$ be the Hankel transforms[4] of $s(r)$ and $h(r)$, respectively. It follows that $H(u,v) = 2\pi\bar{h}(\omega)$ and $S(u,v) = 2\pi\bar{s}(\omega)$ (cf. Papoulis 1981, p. 152), implying $S = S^*$ since $\bar{s}$ is real. From (24),

$$\bar{h}(\omega) = \alpha\bar{s}(\omega)\mathrm{e}^{-i\omega r_0\cos(\theta-\phi)} \ . \qquad \text{(A3)}$$

So the assumption $r_0 > 0$ implies that $\bar{h}$ is complex, from which one may already deduce that only the case $r_0 = 0$ is meaningful. To see that this is indeed the case, let us assume for a moment that $\bar{h}$ is indeed given by (A3). Then $g_t(r)$ is given by

$$g_t(r) = \frac{\alpha}{4\pi^2} \int_0^{\infty} 2\pi\omega\bar{s}(\omega) 2\pi\bar{s}(\omega) \int_{-\pi}^{\pi} \mathrm{e}^{-i\omega r_0\cos(\theta-\phi)} \mathrm{d}\theta \, \mathrm{d}\omega \ ,$$

implying, since

$$J_0(x) = \frac{1}{2\pi} \int_0^{\infty} \mathrm{e}^{i\omega r\cos(\theta-\phi)} \mathrm{d}\theta \ , \qquad \text{(A4)}$$

that

$$g_t(r) = 2\pi\alpha \int_0^{\infty} \omega|\bar{s}(\omega)|^2 J_0((r-r_0)\omega)\mathrm{d}\omega, \quad r \geq r_0 \ . \qquad \text{(A5)}$$

For $r = r_0$ in particular, one has

$$g_t(r_0) = 2\pi\alpha \int_0^{\infty} \omega|\bar{s}(\omega)|^2 \mathrm{d}\omega \ , \qquad \text{(A6)}$$

since $J_0(0) = 1$. So the response on the circle with radius $r_0 > 0$ is the same as in the point $x_0 = y_0 = 0$, i.e. for the case $r_0 = 0$. On the other hand, $J_0(r - r_0)$ is not defined for $r < r_0$, i.e. $g_t(r)$ is not defined for $r < r_0$, implying that the assumption $r_0 > 0$ is not meaningful.

Let s_t now be the stimulus presented in the experiment, and s the pattern resulting from passing s_t through some radially-symmetric filter (the pre-filter) with PSF $h_0(r)$ and corresponding Hankel transform $\bar{h}_0(\omega)$. Let S_t, H_0 and S be the Fourier transforms of s_t, h_0 and s, respectively. Then $S(u,v) = S_t(u,v)H_0(u,v)$, and since $S(u,v) = 2\pi\bar{s}(\omega)$, $H_0(u,v) = 2\pi\bar{h}_0(\omega)$ and $S_t(u,v) = 2\pi\bar{s}_t(\omega)$, it follows that $\bar{s}(\omega) = 2\pi\bar{s}_t(\omega)\bar{h}_0(\omega)$. With $r_0 = 0$ (A3) leads then to

$$g_t(r) = 2\pi\alpha \int_0^{\infty} \omega|\bar{h}_0(\omega)\bar{s}_t(\omega)|^2 J_0(r\omega)\mathrm{d}\omega \ . \qquad \text{(A7)}$$

So g_t is the response of a system or "channel" with system function

$$\bar{h}_t(\omega) = \alpha_0|\bar{h}_0(\omega)|^2\bar{s}_t(\omega), \quad \alpha_0 = 2\pi\alpha \ . \qquad \text{(A8)}$$

$\bar{h}_t$ defines the matched channel for the stimulus pattern s_t.

[4] The Hankel transform of a function $f(r)$ is given by $\bar{f}(\omega) = \int_0^{\infty} rf(r)J_0(\omega r)\mathrm{d}r$.

References

Aertsen AMH, Gerstein MK, Habib MK, Palm G (1989) Dynamics of neuronal firing correlation: modulation of "effective connectivity". J Neurophysiol 61: 900–917

Attneave F (1954) Some informational aspects of visual perception. Psychol Rev 61: 183–193

Barlow HB (1961) The coding of sensory images. In: Thorpe WH, Zangwill OL (eds) Current problems in animal behavior. Cambridge University Press, Cambridge

Barlow HB (1983) Understanding natural vision. In: Braddick OJ, Sleigh AC (eds) Physical and biological processes of images. (Springer Series of Information Sciences, vol 11), Springer, Berlin Heidelberg New York, pp 2–14

Barth E, Zetzsche C, Rentschler I (1998) Intrinsic two-dimensional features as textons. J Opt Soc Am A 15: 1723–1732

Bauer R, Dicke P (1997) Fast cortical selection: a principle of neuronal self-organization for perception? Biol Cybern 77: 207–215

Campbell FW, Robson JG (1968) Application of Fourier analysis to the visibility of gratings. J Physiol (Lond) 197: 551–566

Field DJ (1987) Relations between the statistics of natural images and the response properties of cortical cells. J Opt Soc Am A 4: 2379–2394

Gerstner W, Ritz R, van Hemmen JL (1993) Why spikes? Hebbian learning and retrieval of time-resolved excitation patterns. Biol Cybern 69: 503–515

Gilbert C, Ito M, Kapadia M, Westheimer G (2000) Interactions between attention, context and learning in primary visual cortex. Vision Res 40: 1217–1226

Graham N (1977) Visual detection of aperiodic spatial stimuli by probability summation among narrowband channels. Vision Res 17: 637–652

Graham N (1989) Visual pattern analysers. Oxford University Press, Oxford

Hauske G (1974) Adaptive filter mechanisms in human vision. Kybernetik 16: 227–237

Hauske G, Lupp U, Wolf W (1978) Matched filters – a new concept in vision. Photogr Sci Eng 20: 59–64

Hauske G, Wolf W, Lupp U (1976) Matched filters in human vision. Biol Cybern 22: 181–188

Hines M (1976) Line spread variation near the fovea. Vision Res 14: 567–572

Hubel DH, Wiesel TN (1968) Receptive fields and functional architecture of monkey striate cortex. J Physiol (Lond) 195: 215–243

Kelly DH, Magnuski HS (1975) Pattern detection and the two-dimensional Fourier transform: circular targets. Vision Res 15: 911–915

Kistler WM, van Hemmen JL (1999) Short-term synaptic plasticity and network behavior. Neural Comput 11: 1579–1594

Kulikowski JJ, King-Smith PE (1973) Spatial arrangement of line, edge and grating detectors revealed by subthreshold summation. Vision Res 13: 1455–1478

Linsker R (1986a) From basic network principles to neural architecture: emergence of spatial-opponent cells. Proc Natl Acad Sci USA 83: 7508–7512

Linsker R (1986b) From basic network principles to neural architecture: emergence of orientation-selective cells. Proc Natl Acad Sci USA 83: 8390–8394

Logvinenko AD (1993) Lack of convexity of threshold curves for compound grating: implications for modelling visual pattern detection. Biol Cybern 70: 55–64

Martinez-Trujillo JC, Treue S (2000) Attention modulates apparent stimulus contrast in the superior temporal sulcus of the macaque monkey. In: Bülthoff HH, Fahle M, Gegenfurtner KR, Mallot HA (eds) Beiträge zur 3. Tübinger Wahrnehmungskonferenz. Knirsch, Kirchentellinsfurth

Meinhardt G (1999) Evidence for different nonlinear summation schemes for lines and gratings at threshold. Biol Cybern 81: 263–277

Meinhardt G (2000) Detection of compound spatial patterns: further evidence for different channel interactions. Biol Cybern 82: 269–282

Meinhardt G, Mortensen U (1998) Detection of aperiodic test patterns by pattern specific detectors revealed by subthreshold summation. Biol Cybern 79: 413–425

Mortensen U, Nachtigall C (2000) Visual channels, Hebbian assemblies and the effect of Hebb's rule. Biol Cybern 82: 401–413

Oja E (1982) A simplified neuron model as a principal component analyzer. J Math Biol 15: 267–273

Papoulis A (1981) Systems and transforms with applications in optics. Krieger, Malabar, Fla

Quick RF (1974) A vector-magnitude model for contrast detection. Kybernetik 16: 65–67

Ritz R, Gerstner W, Fuentes U, van Hemmen JL (1994) A biologically motivated and analytically soluble model of collective oscillations in the cortex. II Application to binding and pattern segmentation. Biol Cybern 71: 349–358

Saito H, Tanaka K, Fukada Y, Oyamada H (1988) Analysis of Discontinuity in visual contours in Area 19 of the cat. Neurosci 8: 1131–1143

Sanger TD (1989) Optimal unsupervised Learning in a single-layer-linear feedforward neural network. Neural Netw 2: 459–473

Sanger TD (1990) Analysis of the two-dimensional receptive fields learned by the generalized Hebbian algorithm in response to random input. Biol Cybern 63: 221–228

van Hateren JH (1992) Real and optimal neural images in early vision. Nature 360: 68–70

Wilson HR (1978) Quantitative prediction of line spread function measurements: implication for channel bandwidths. Vision Res 18: 493–496

Wilson HR, Bergen JR (1979) A four mechanism model of threshold spatial vision. Vision Res 19: 515–522

Wilson HR, Levi D, Maffei L, Rovamo J, DeValois R (1990) The perception of form: retina to striate cortex. In: Spillmann L, Werner JS (eds) Visual perception. The neurophysiological foundations. Academic Press, San Diego, pp 231–272

Zetzsche C, Barth E (1990) Fundamental limits of linear filters in the visual processing of two-dimensional signals. Vision Res 30: 1111–1117

Zetzsche, C, Barth E, Wegmann B (1993) The importance of intrinsically two-dimensional image features in biological vision and picture coding. In: Watson AB (ed) Digital images and human vision. MIT Press, Cambridge, Mass

Zetzsche C, Krieger G (1999) Nonlinear neurons and higher-order statistics: new approaches to human vision and electronic image processing. In: Rogowitz B, Pappas TV (eds) Human vision and electronic imaging IV. Proc SPIE vol 3644. SPIE, Bellingham Wassh, pp 2–33